A Journal of the Gesellschaft Deutscher Chemiker

Angewandte International Edition

GDCh

Chemie

www.angewandte.org

Accepted Article

Title: Selenium-Modified Microgels as Bio-Inspired Oxidation Catalysts

Authors: Kok Hui Tan, Wenjing Xu, Simon Stefka, Dan Demco, Tetiana Kahrandiuk, Volodymyr Ivasiv, Roman Nebesnyi, Vladislav Petrovskii, Igor Potemkin, and Andrij Pich

To be cited as: *Angew. Chem. Int. Ed.* 10.1002/anie.201901161
Angew. Chem. 10.1002/ange.201901161

Link to VoR: http://dx.doi.org/10.1002/anie.201901161
http://dx.doi.org/10.1002/ange.201901161

WILEY-VCH

10.1002/anie.201901161

WILEY-VCH

Selenium-Modified Microgels as Bio-Inspired Oxidation Catalysts

Kok H. Tan, Wenjing Xu, Simon Stefka, Dan E. Demco, Tetiana Kharandiuk, Volodymyr Ivasiv, Roman Nebesnyi, Vladislav S. Petrovskii, Igor I. Potemkin, and Andrij Pich*

Abstract: Active colloidal catalysts inspired by the glutathione peroxidase (GPx) were synthesized by integration of catalytically active selenium (Se) moieties into aqueous microgels. Diselenide crosslinker (Se X-linker) was successfully synthesized and incorporated into microgels through precipitation polymerization, along with conventional crosslinker *N,N´*-Methylenebis(acrylamide) (BIS). Diselenide bonds inside the microgels were cleaved through oxidation by H_2O_2 and converted to seleninic acid whilst maintaining the microgel microstructure intact. Using this approach catalytically active microgels with variable amounts of seleninic acid were synthesized. Remarkably, the microgels exhibited higher catalytic activity and selectivity at low reaction temperatures compared with the molecular Se catalyst in a model oxidation reaction of acrolein to acrylic acid and methyl acrylate.

The importance of catalysts is testified by its applications, use in most biological reactions,[1] industrial syntheses[2] as well as environmental protection.[3] Heterogeneous catalysts cover the majority of catalysis applications, providing the advantage to ease the processing and separation after the reactions. However, the heterogeneity contributes to the inferiority in catalytic activity and, therefore, tremendous research efforts were devoted recently by merging heterogeneous and homogeneous catalysts by immobilizing catalysts onto colloidal supports. Hence, providing high catalytic efficiency (activity and selectivity) and easy separation for catalyst recycling and re-use.[4] Up until recently, the majority of colloidal supports used in heterogeneous catalysts were metal oxides,[5] zeolites[6] or polymers.[7]

Microgels are porous particles consisting of a crosslinked polymeric network, forming colloidally-stable dispersions that swell in water and other solvents.[8] Microgels can be tailored to possess unique properties enabling them to respond to external stimuli such as temperature,[9] ionic strength,[10] pH,[11] pressure,[12] electric potential,[13] and light.[14] Owing to their biocompatibility and chemical diversity, microgels are utilized in biological applications ranging from controlled drug delivery,[15] scaffolding for cell proliferation,[16] biosensors,[17] to biocatalysts.[18]

Poly(*N*-vinylcaprolactam) (PVCL) microgels have attracted much attention because of their chemical stability, bio-compatibility, and stimuli-responsiveness. PVCL microgels exhibit *volume phase transition temperature* (VPTT) around 32 °C that is close to physiological temperature. The temperature-triggered swelling/deswelling behavior of PVCL microgels allows for the controlling of their mesh size and solvent permeability. Therefore PVCL microgels have been discussed as promising materials in catalysis,[19] biology or biomedical applications.[20]

In particular, the application of microgels in catalysis may open attractive possibilities for the design of new interactive catalyst systems. Several studies reported that microgels can allow guest molecules to diffuse into the porous polymeric network during swelling, where the molecules will then be trapped inside the microstructure during collapsing of the network. Subsequent swelling of the microgels releases the guest molecules.[21] Furthermore, computer simulations have demonstrated that polymeric microgels reduce the surface tension of interface between two immiscible liquids by spreading at the interface promoting the mixing of incompatible liquids within the polymeric network.[22] The microgels act as a "compatibilizer" and could be useful for the development of stimuli responsive systems for interfacial catalysis.[23] Considering these extraordinary properties, microgels have also been used as functional carriers for catalytically-active nanoparticles,[24] organometallic catalysts,[25] and organocatalysts.[26]

Since the discovery of selenium functions in biological systems,[27] much attention has been devoted to elucidating the importance of selenium in selenoenzymes.[28] Glutathione peroxidase (GPx), an enzyme with antioxidation properties, can be found in most mammals.[29] The unique structure of the selenocysteine as the active center within the protein structure enables the catalytic oxidation/reduction reaction to be carried out.[30] Decades of research has been carried out to produce materials that mimic the glutathione peroxidase (GPx).[31] For the efficient mimicking of the protein structure, a three-dimensional (3D) porous structure is required, which is responsible for the fixation of the active Se-groups and provides a compartmentalized environment to promote the diffusion of reagents for the catalytic reactions to occur. Several polymer structures containing selenium e.g., supramolecular micelles,[32] dendrimers,[33] hyperbranched polymers,[34] and nanogels[35] have been discussed in the literature. However, the majority of the developed systems utilize the redox properties of the selenium atom for drug delivery applications. The use of Se-modified functional polymer architectures as bio-inspired catalysts has not been intensively explored so far.

[*] K. H. Tan, S. Stefka, W. Xu, Prof. D. E. Demco, Prof. I. I. Potemkin, Prof. A. Pich
DWI Leibniz Institute for Interactive Materials e.V.,
RWTH Aachen University
Forckenbeckstraße 50, 52074 Aachen, Germany
E-mail: pich@dwi.rwth-aachen.de
T. Kharandiuk, Dr. R. Nebesnyi, Dr. V. Ivasiv
Technology of Organic Products Department, Lviv Polytechnic National University, Stepana Bandery str. 12, 79013, Ukraine
Prof. D. E. Demco
Technical University of Cluj-Napoca, Department of Physics and Chemistry, RO-400027 Cluj-Napoca, Romania
V. S. Petrovskii, Prof. I. I. Potemkin
Physics Department, Lomonosov Moscow State University, Leninskie Gory 1-2, Moscow 119991, Russian Federation
Prof. I. I. Potemkin
National Research South Ural State University, Chelyabinsk 454080, Russian Federation
Prof. A. Pich
Aachen Maastricht Institute for Biobased Materials (AMIBM), Maastricht University, Urmonderbaan 22, 6167 RD Geleen, The Netherlands

Supporting information and the ORCID identification number(s) for the author(s) of this article can be found under:

10.1002/anie.201901161

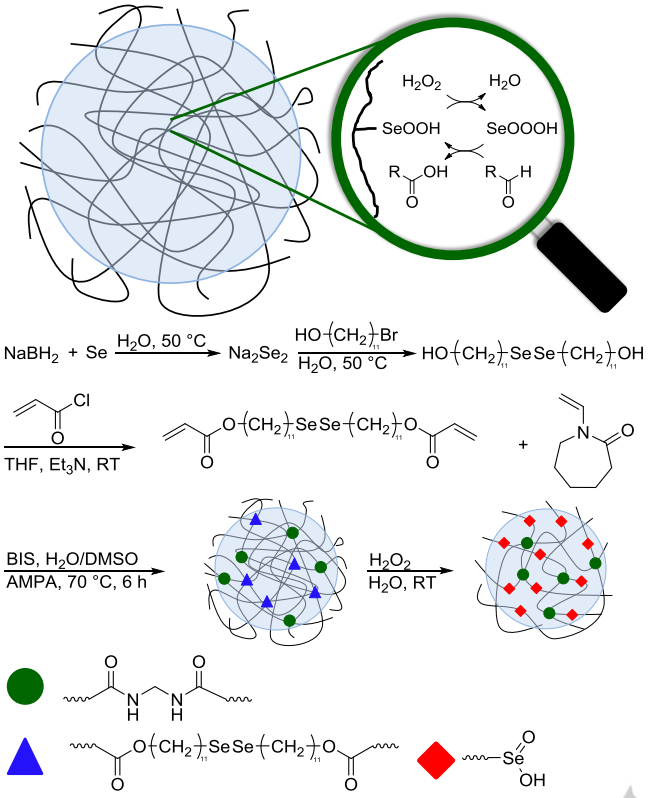

Scheme 1. Selenium modified microgels as a catalyst for the oxidation of aldehydes followed by the synthetic routes of diselenide crosslinker (Se X-linker) and the incorporation of Se X-linker to the PVCL microgels simultaneously with BIS as the permanent crosslinker. The microgels can be oxidized by H_2O_2 resulting the transformation of diselenide groups into seleninic acid groups.

Herein, we attempt to take advantage of the microenvironment provided by the 3D polymer network structure of the PVCL microgels to introduce selenium functional groups as the catalytic centers in order to achieve GPx-like activity. For this purpose, we first performed a three-step synthesis to obtain the diselenide crosslinker (Scheme 1). The diselenide crosslinker was then incorporated into PVCL microgels by conventional precipitation polymerization together with a permanent crosslinker (BIS). After cleavage of the diselenide bonds by H_2O_2, microgels modified with seleninic acid were obtained (Scheme 1).

The synthesized diselenide crosslinker was characterized by IR and Raman spectroscopy as well as ^{1}H and ^{77}Se NMR spectroscopy. IR spectra proved that after conjugation of the 11-bromoundecanol onto diselenide, an increase in hydroxyl group signal intensity at an absorbance band of 3431 cm^{-1} and 3371 cm^{-1} was observed (Figure S1 of Supporting Information). In Raman spectra, the symmetrical stretching vibration of diselenide (SeSe) bond gives rise to a strong polarized band. The diselenide characteristic band can be observed at 294 cm^{-1} (Figures 1b and S2 of Supporting Information). After acrylation of bis(11-hydroxyundecyl) diselenide, new absorbance bands in IR spectra can be observed at 1726 cm^{-1}, 1192 cm^{-1} and 984 cm^{-1} corresponding to carbonyl group stretching, C-O-C stretching in ester and to the CH=CH$_2$ out-of-plane deformation (Figure S1 of Supporting Information).

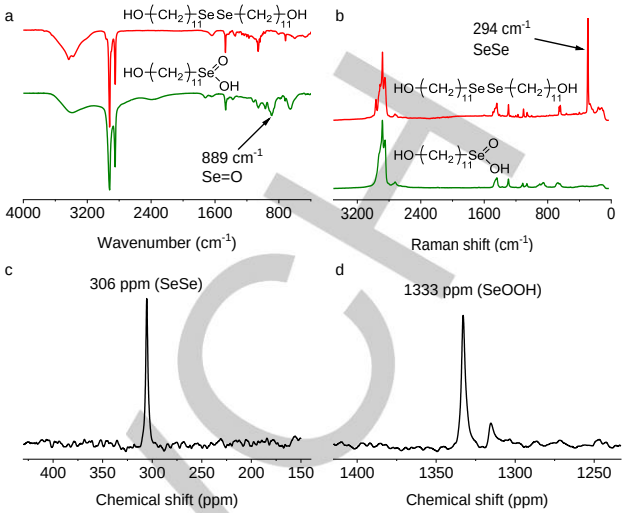

Figure 1. (a) IR spectra and (b) Raman spectra of bis(11-hydroxyundecyl) diselenide before (red) and after (green) oxidation by H_2O_2; ^{77}Se NMR of bis(11-acryloyloxyundecyl) diselenide (c) before and (d) after oxidation by H_2O_2.

To optimize the oxidative cleavage of the diselenide bond, bis(11-hydroxyundecyl) diselenide was chosen as the model molecule. Upon oxidation by H_2O_2, diselenide bonds were cleaved and the compound was characterized by IR, Raman, and ^{77}Se NMR spectroscopy. A new strong absorbance band at 889 cm^{-1} (Figure 1a), and a moderate signal at 859 cm^{-1} (Figure 1b) were observed in IR and Raman spectra, respectively, corresponding to the Se=O stretching, proving the diselenide was cleaved and oxidized to seleninic acid. Also, the diselenide signal at 294 cm^{-1} disappeared completely after oxidation (Figure 1b). From ^{77}Se-NMR shown in Figure 1c and 1d, the peak shifted from 306 ppm to 1333 ppm after oxidation,

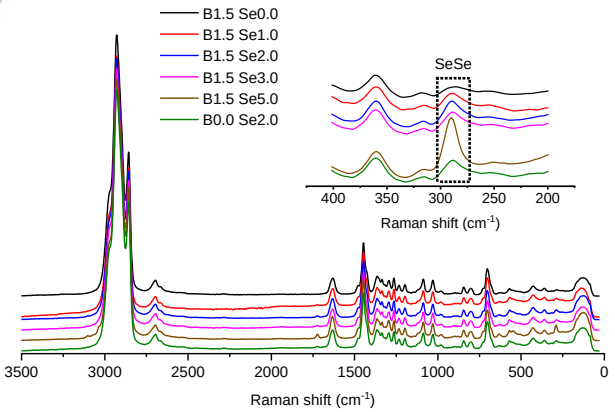

Figure 2. Raman spectra of Se-modified microgels with a constant amount of (BIS) crosslinker and a variable amount of diselenide crosslinker (0.0 to 5.0 mol%). Microgels synthesized without (BIS) but with 2.0 mol% diselenide crosslinker were synthesized as a control sample. The intensities of the peak at 2928 cm^{-1} were normalized. In the inset, the enhanced spectra showed the signal related to the diselenide bond at around 290 cm^{-1}.

indicating the diselenide was cleaved and converted to seleninic acid. The peak at 1316 ppm could be from the partial amount of selenium derivative with a lower oxidation state. ^{1}H NMR spectra

of the diselenide crosslinker synthesis and after oxidation by 1 wt% H_2O_2 can be found in the Supporting Information (Figures S3-S6).

Poly(*N*-vinylcaprolactam) (PVCL) microgels with diselenide groups were synthesized by precipitation polymerization in aqueous media at 70°C (Scheme 1). A small amount of DMSO (10 v/v%) was added to water to improve the solubility of the hydrophobic diselenide crosslinker during the polymerization process. Higher amounts of DMSO used in the reaction mixture led to the inhibition of microgel formation, probably due to the fact that growing PVCL chains lose the ability to precipitate due to the shift of lower critical solution temperature (LCST) to higher values.[36] The microgels containing diselenide crosslinker were obtained in the form of colloidally stable dispersions. Series of selenium-containing PVCL microgels with different diselenide amounts were synthesized and some important characteristics are shown in Table 1. Raman spectra of the series of selenium-containing PVCL microgels were measured to characterize the incorporation of diselenide crosslinker into the microgels. The highest amount of incorporated SeSe was obtained in B1.5 Se5.0 (Figure 2).

Table 1. Selenium containing PVCL microgels with a fixed amount of BIS with variable amounts of incorporated diselenide crosslinker.

Sample	VCL/g	BIS/mol%[a]	Se X-linker/mol%[a]	Yield/%[b]
B1.5 Se0.0	1.0	1.5	0.0	82
B1.5 Se1.0	1.0	1.5	1.0	76
B1.5 Se2.0	1.0	1.5	2.0	84
B1.5 Se3.0	1.0	1.5	3.0	65
B1.5 Se5.0	1.0	1.5	5.0	69
B0.0 Se2.0	1.0	0.0	2.0	73

[a] Ratio of the mol of each crosslinker over the mol of VCL & [b] Dried weight of lyophilized microgels over the VCL input

Next, the oxidation of diselenide bonds in microgels was investigated. Three selected microgels (B1.5 Se0.0, B1.5 Se2.0, and B0.0 Se2.0) were incubated with 1.0 wt% H_2O_2 overnight. The degraded microgels were characterized by dynamic light scattering, Raman spectroscopy, and electron microscopy. Figure 3 depicts the probability distribution curves of the selected microgels. For microgels containing only BIS as the crosslinker, negligible changes in the hydrodynamic radius after treatment with H_2O_2 were observed (Figure 3a). However, a significant reduction of the hydrodynamic radius can be detected for microgel sample B0.0 Se2.0 containing only diselenide crosslinks (Figure 3c). These results are consistent with results presented in Figure 1 and prove that upon oxidation by H_2O_2, diselenide bonds were cleaved and oxidized to seleninic acid. This leads to the change of the network topology and degradation of microgels to water-soluble PVCL chains as reflected in the strong reduction of the hydrodynamic radius. As expected, microgel sample B1.5 Se2.0, which contains both cleavable diselenide crosslinks and non-cleavable BIS crosslinks showed only a slight reduction of the hydrodynamic radius after oxidation (Figure 3b). Such behavior can be explained by a presence of hydrophobic alkyl groups in diselenide crosslinker. Before oxidation, the alkyl double spacer is strained connecting PVCL subchains. We can imagine that the hydrophobic nature of the crosslinkers does not play a role in this state: they cannot aggregate with each other and hydrophobic units of PVCL which would be accompanied by high elastic stress. On the contrary, after oxidation (i) two spacers of each cleaved crosslinker get more degrees of the freedom, (ii) the microgel becomes softer (less total number of cross-linkers) and the spacers can aggregate with each other and hydrophobic units of the PVCL without strong elastic penalty of the network forming hydrophobic domains which result is compaction of the microgels. The aggregation of the alkyl chains with each other and PVCL chains is demonstrated in Figure S7 and Movie 1 using all-atomistic molecular dynamics simulations. Optical images of microgel dispersions were captured before and after degradation of the microgels. It can be seen that microgels with only BIS crosslinks remain turbid after oxidation (Figure 3d) but in the case of microgel sample B0.0 Se2.0, the solution turned from turbid to clear (Figure 3f). This indicates that the dispersed microgels were degraded into water soluble PVCL chains.

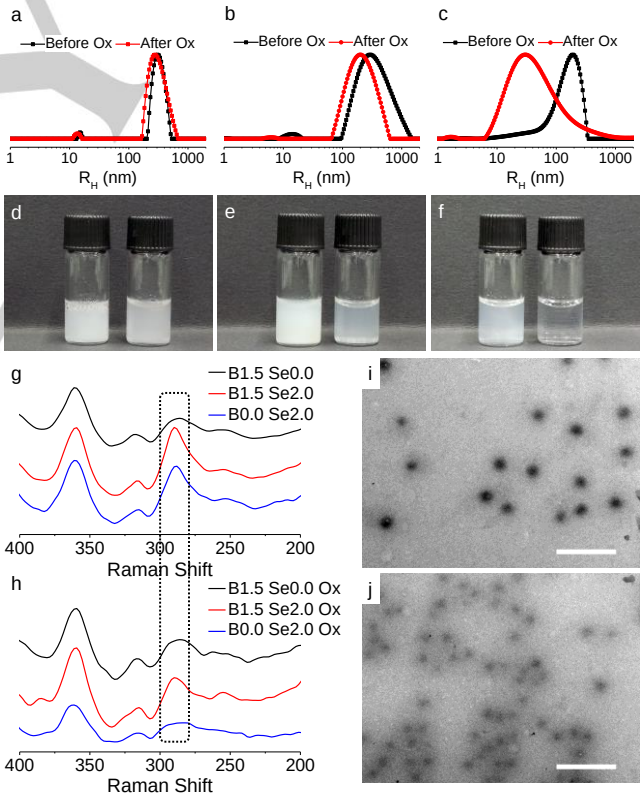

Figure 3. Probability distribution curves generated by Inverse Laplace Transform of $g_2(t)$ exponential correlation function of selenium containing PVCL microgels before and after oxidation by H_2O_2 (a) B1.5 Se0.0, (b) B1.5 Se2.0, (c) B0.0 Se2.0. The photos (left: before oxidation; right: after oxidation) of (d), (e), and (f) correspond to (a), (b), and (c), respectively. Raman spectra of BIS 1.5% SeSe 2.0% (g) before and (h) after oxidation by H_2O_2. TEM images of B1.5 Se2.0 (i) before and (j) after oxidation by H_2O_2 (scale bar is 1000 nm).

In the case of microgel sample B1.5 Se2.0, the turbidity was partially reduced after oxidation due to the reduction of the scattering intensity originating from reduced density of polymer chains within microgels (Figure 3e). The hydrodynamic radii of microgel samples before and after oxidation with H_2O_2 are summarized in Table 2. The hydrodynamic radii of microgels measured at 50°C are smaller due to the fact that microgels collapse above their VPTT. These experimental results

Table 2. Hydrodynamic radii (R_H) of microgels before and after oxidation by H_2O_2.

Sample	Before oxidation/R_H		After oxidation/R_H	
	20 °C (nm)	50 °C (nm)	20 °C (nm)	50 °C (nm)
B1.5 Se0.0	286	105	284	102
B1.5 Se2.0	192	87	179	91
B0.0 Se2.0	131	40	32	32

indicate that the incorporation of Se into microgels is not influencing the temperature-responsiveness of microgels in aqueous solution but rather the transition temperature.

Raman spectra for the selected microgels were measured after the oxidation process and compared with those collected before oxidation (Figure 3). The diselenide absorbance band observed reduced significantly showing the diselenide bonds in the microgels networkwere cleaved (Figure 3g & 3h). ^{77}Se NMR of oxidized B0.0 Se2.0 depicts the typical seleninic acid peak at 1050 ppm (Figure S8). STEM images of microgel sample B1.5 Se2.0 showed core-shell morphology before (Figure S9a) and after oxidation (Figure S9b). This can be explained by the higher reactivity of BIS[37] compared with VCL and diselenide crosslinker. Therefore, a microgel core contains more crosslinks and a denser network structure compared to the shell. According to TEM images (Figure 3i & 3j), the microgels B1.5 Se2.0 before oxidation have an average diameter of 268 nm and after oxidation an average diameter of 236 nm. The reduced microgel sizes are due to the drying effect during TEM sample preparation. However, the structure of the microgels remains intact. TEM images of microgel samples B1.5 Se0.0 and B0.0 Se2.0 before and after oxidation are shown in Figures S10 and S11.

In the next step, the catalytic activity of selenium containing microgels was evaluated in the oxidation of acrolein as a model reaction (Figure 4a). The oxidation reactions were performed in methanol and dioxane at 50 °C up to 24 hours reaction time with constant catalyst concentration (Se-unit concentration for microgels and Se X-linker was 0.0044 mol/L. For PVCL its mass was the same as for Se 2.0 microgel) in all reactions. As proved by dynamic light scattering, PVCL microgels lose their temperature-responsive properties in MeOH and dioxane, but remain fully swollen and colloidally stable (Supporting Information, Figure S12).[38] The control reactions were performed using the diselenide crosslinker and the PVCL microgel without Se. The oxidation of acrolein using Se-catalysts led to the formation of both methyl acrylate and acrylic acid in methanol solution and only acrylic acid in dioxane solution.

Figures 4b and S13 depict the overall catalytic results obtained for the methanol-water mixture. All selenium-containing microgels and Se-X-linker show a much higher selectivity towards methyl acrylate compared with acrylic acid (ester/acid ratio is 0.9-0.95).

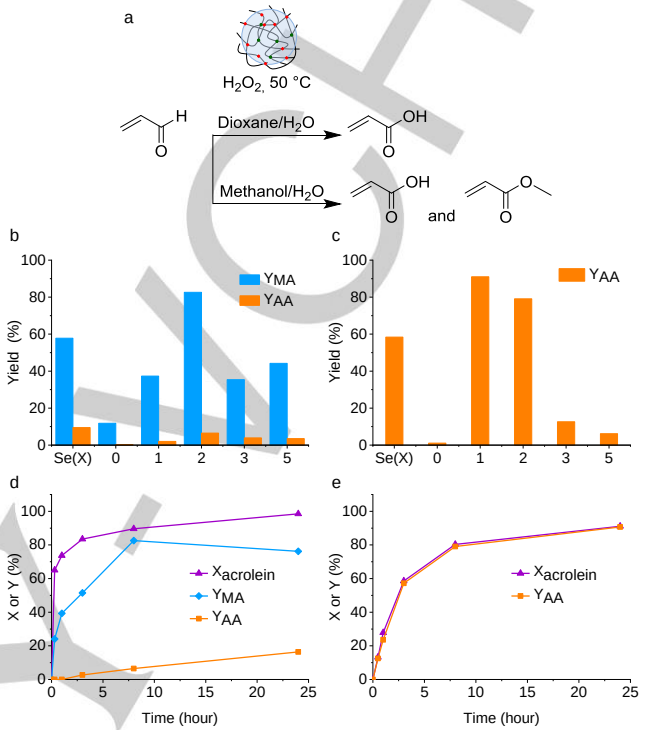

Figure 4. a) The reaction scheme of the oxidation of acrolein by H_2O_2 catalyzed by selenium containing PVCL microgels resulting in acrylic acid (AA) and methyl acrylate (MA). Oxidation of acrolein catalyzed by the selenium crosslinker (Se(X)) and the series of selenium containing PVCL microgels with BIS 1.5 mol% after 8 hours reaction yielded b) methyl acrylate (MA) and acrylic acid (AA) in methanol-H_2O medium and c) acrylic acid in dioxane-H_2O medium. The catalytic yield after 24 hours reaction d) and e) correspond to b) and c), respectively. Y is the yield and $X_{acrolein}$ is the conversion of acrolein.

As such, Se-microgels can be used for the selective synthesis of methyl acrylate as a primary product. Comparatively, in an oxidation reaction of unsaturated aldehydes with H_2O_2 as the oxidant and H_2SeO_3 as the catalyst in methanol medium under similar reaction conditions, the ester/acid ratio is 0.3-0.5,[39] which indicates probable differences in the reaction mechanism between selenous acid and seleninic acid groups in the microgel.

Among tested catalysts maximum total yield of methyl acrylate and acrylic acid (89.1 %) was achieved with B1.5 Se2.0 microgel, which is much higher than for Se-X-linker (67.3 %) and other Se-microgels. It should be noted that non-catalytic reaction also occurs with acrylates yield up to 12 % as indicated by performing the reaction with PVCL microgel without Se. B1.5 Se1.0, B1.5 Se3.0, and B1.5 Se5.0 microgels demonstrate lower methyl acrylate and acrylic acid yields compared with B1.5 Se2.0. In the case of the B1.5 Se1.0 microgel, this can be caused by lower diffusion rates of the reagents as a result of the higher viscosity of the reaction mixture (the highest amount of microgel was used due to the lowest content of Se-units). In the case of the B1.5 Se3.0 and B1.5 Se5.0 microgels lower yields can be attributed to reduced reaction volume, as the reaction primarily occurs inside of the microgel particles, and, considering

that average Se concentration was kept constant for all microgels, higher Se content inside the microgel means lower total volume of microgel particles.

Best results were achieved when the reaction time was 8 hours (Figure 4d). Further increases in reaction time results in a decrease of methyl acrylate yield and an increase of acrylic acid yield. This can be caused by methyl acrylate hydrolysis to acrylic acid as the concentration of water increases during the reaction due to water formation as a by-product. Therefore, 8 hours of reaction time can be assumed as optimum for methyl acrylate synthesis.

As it was mentioned above in the case of dioxane-water mixture the only desired product is acrylic acid (Figure 4c and S13). But the maximum yield of acrylic acid (91.0 %) was achieved with B1.5 Se1.0 microgel, which is also much higher than for Se X-linker (58.4 %). With B1.5 Se2.0 microgel a similar acrylic acid yield was achieved (79.1 %), but B1.5 Se3.0 and B1.5 Se5.0 microgels have a much lower catalytic activity. In the case of dioxane solution non-catalytic reaction (the reaction with PVCL microgel without Se) practically does not occur and only traces of acrylic acid are formed after 8 hours of the reaction. It is worth mentioning that the oxidation of acrolein in dioxane solution occurs with very high selectivity for acrylic acid – nearly 99 % (Figure 4e). As mentioned above acrylic acid yield after 8 hours of the reaction is 79.1 % with B1.5 Se2.0 microgel; further increase of reaction time leads only to the minor increase of acrylic acid yield (90.7 % after 24 hours). Based on the TOF values (h^{-1}) (Table S2), synthesized microgels and Se X-linker can be placed in the following ranges: Se 2.0 (50.6) > Se X-linker (41.2) > Se 5.0 (27.0) > Se 3.0 (24.1) > Se 1.0 (22.4) for methanol-water media; Se 1.0 (51.7) > Se 2.0 (44.9) > Se X-linker (33.2) > Se 3.0 (7.1) > Se 5.0 (3.4) for dioxane-water media.

There are also reported results of acrolein oxidation with Au/ZnO catalyst and air as an oxidant under similar reaction conditions.[40] Methyl acrylate yield was 30 % at 8 hours and 84 % at 50 hours. Furthermore, acrolein oxidation reaction was performed in a gas phase with MoVTeNb as the catalyst.[41] Methyl acrylate yield was 78 %, which is lower than in our work, and the reaction temperature was much higher at 250 °C. Compared with these results on non-Se catalysts,[40-41] using B1.5 Se2.0 microgel facilitates a similar methyl acrylate yield but at a significantly lower reaction time and under milder reaction temperatures. In preliminary experiments, we could demonstrate that selenium modified microgels can be used in a consecutive oxidation run (Supporting Information, Figure S14) without considerable loss of their activity. By adding new reagents (acrolein and hydrogen peroxide) to the system after first catalytic cycle (24 hours), the formation of acrylic acid was observed with slightly lower yield (Figure S14). The lower acrylic acid yield after second and third catalytic cycles are associated with the presence of a high amount of acrylic acid in the reaction volume (acrylic acid is constantly formed during the reaction, the second and third cycles were performed without preliminary products separation). High acrylic acid concentration affects the equilibrium of the reaction, the increase of reaction mixture viscosity and leads to the deterioration of the diffusion process. Nevertheless, selenium-modified microgels remain catalytically active even after 72 h of reaction and we believe that selenium-modified microgels can be recycled and used efficiently in many catalytic cycles.

In conclusion, selenium-containing microgels were successfully synthesized and characterized. The diselenide groups within the microgels were able to be oxidized and cleaved into seleninic acid groups while maintaining the microstructure of microgels. Se-modified microgels were successfully used as colloidal catalysts in the model reaction of the oxidation of acrolein to acrylic acid and methyl acrylate. We demonstrate that the selenium moieties in the microgels exhibit high catalytic activity reflected in favorable catalytic yields and selectivities. In addition, microgel samples B1.5 Se1.0 and B1.5 Se2.0 exhibit exceptional catalytic activity compared with the diselenide crosslinker and other reported results. This study indicates that Se-modified PVCL microgels could be potentially used as efficient catalysts for various oxidation processes. In addition, the use of Se-modified PVCL microgels as catalysts in aqueous solutions will allow exploring the influence of their temperature-induced swelling-deswelling on the catalytic activity. Synthesized Se-modified microgels can catalyze oxidation reactions with high activity and selectivity at mild temperatures, which allows for a considerable reduction of the energy consumption in technical processes. The biocompatibility of microgels unleashes an attractive possibility for their use in biomedical applications as redox-triggered drug carriers or scavengers for reactive oxygen species (ROS) and cell protection from oxidative stress.

Acknowledgments

The authors acknowledge Volkswagen Stiftung for the project A115859 funding. Authors thank SFB 985 “Functional Microgels and Microgel Systems” for financial support. The financial support of the Government of Russian Federation within Act 211, Contract 02.A03.21.0011, and the Russian Foundation for Basic Research, project No. 19-03-00472, is gratefully acknowledged. The computer simulations were carried out using the equipment of the shared research facilities of HPC computing resources at Lomonosov Moscow State University. The authors also thank Dr. Walter Tillmann for the FTIR and Raman spectroscopy measurements and many thanks to Lindsey Weger for proofreading the manuscript.

Conflict of interest

The authors declare no conflict of interest.

Keywords: microgels • selenium • redox chemistry • organocatalysis

[1] G. M. Cooper, R. E. Hausman, in *The Cell: A Molecular Approach*, ASM Press, Washington, D.C., **2007**, pp. 73.

[2] J. Hagen, in *Industrial Catalysis*, 3rd Edition ed., Wiley-VCH Verlag GmbH & Co. KGaA, Weinheim, Germany, **2015**, pp. 459.

[3] C. Han, E. Sahle-Demessie, A. Shah, S. Nawaz, L.-u. Rahman, N. B. McGuinness, S. C. Pillai, H. Choi, D. D. Dionysiou, M. N. Nadagouda, in *Sustainable Catalysis* (Eds.: R. Luque, F. L.-Y. Lam), Wiley-VCH, Weinheim, Germany, **2018**.

[4] J. Hagen, in *Industrial Catalysis*, 3rd Edition ed., Wiley-VCH Verlag GmbH & Co. KGaA, Weinheim, Germany, **2015**, pp. 1.

[5] a) S. F. J. Hackett, R. M. Brydson, M. H. Gass, I. Harvey, A. D. Newman, K. Wilson, A. F. Lee, *Angew. Chem. Int. Ed.* **2007**, *46*, 8593; *Angew. Chem.* **2007**, *119*, 8747; b) B. T. Qiao, A. Q. Wang, X. F. Yang, L. F. Allard, Z. Jiang, Y. T. Cui, J. Y. Liu, J. Li, T. Zhang, *Nat. Chem.* **2011**, *3*, 634; c) B. T. Qiao, J. X. Liang, A. Q. Wang, C. Q. Xu, J. Li, T. Zhang, J. Y. Liu, *Nano Res.* **2015**, *8*, 2913.

[6] a) M. E. Davis, *Acc. Chem. Res.* **1993**, *26*, 111; b) R. A. Sheldon, *J. Mol. Catal. A: Chem.* **1996**, *107*, 75.

[7] a) Y.-S. Hon, C.-F. Lee, R.-J. Chen, P.-H. Szu, *Tetrahedron* **2001**, *57*, 5991; b) Y. Masaki, T. Yamada, N. Tanaka, *Synlett* **2001**, *2001*, 1311.

[8] a) F. A. Plamper, W. Richtering, *Acc. Chem. Res.* **2017**, *50*, 131; b) R. Pelton, T. Hoare, in *Microgel Suspensions* (Eds.: A. Fernandez-N., H. Wyss, J. Mattsson, D. A. Weitz), Wiley-VCH Verlag GmbH & Co. KGaA, **2011**, pp. 1; c) A. Pich, W. Richtering, in *Chemical Design of Responsive Microgels*, Springer Berlin Heidelberg, **2010**.

[9] L. A. Lyon, Z. Y. Meng, N. Singh, C. D. Sorrell, A. S. John, *Chem. Soc. Rev.* **2009**, *38*, 865.

[10] a) H. Kobayashi, R. G. Winkler, *Polymers* **2014**, *6*, 1602; b) H. Kobayashi, R. G. Winkler, *Sci. Rep.* **2016**, *6*, 19836.

[11] a) A. A. Polotsky, F. A. Plamper, O. V. Borisov, *Macromolecules* **2013**, *46*, 8702; b) A. A. Rudov, A. P. H. Gelissen, G. Lotze, A. Schmid, T. Eckert, A. Pich, W. Richtering, I. I. Potemkin, *Macromolecules* **2017**, *50*, 4435.

[12] S. Grobelny, C. H. Hofmann, M. Erlkamp, F. A. Plamper, W. Richtering, R. Winter, *Soft Matter* **2013**, *9*, 5862.

[13] O. Mergel, P. Wunnemann, U. Simon, A. Boker, F. A. Plamper, *Chem. Mater.* **2015**, *27*, 7306.

[14] a) D. I. Phua, K. Herman, A. Balaceanu, J. Zakrevski, A. Pich, *Langmuir* **2016**, *32*, 3867; b) C. D. Vo, D. Kuckling, H. J. P. Adler, M. Schohoff, *Colloid. Polym. Sci.* **2002**, *280*, 400.

[15] a) C. M. Nolan, M. J. Serpe, L. A. Lyon, *Biomacromolecules* **2004**, *5*, 1940; b) M. J. Serpe, K. A. Yarmey, C. M. Nolan, L. A. Lyon, *Biomacromolecules* **2005**, *6*, 408; c) I. Lynch, P. de Gregorio, K. A. Dawson, *J. Phys. Chem. B* **2005**, *109*, 6257.

[16] a) C. M. Nolan, C. D. Reyes, J. D. Debord, A. J. Garcia, L. A. Lyon, *Biomacromolecules* **2005**, *6*, 2032; b) A. W. Bridges, N. Singh, K. L. Burns, J. E. Babensee, L. A. Lyon, A. J. Garcia, *Biomaterials* **2008**, *29*, 4605.

[17] L. V. Sigolaeva, S. Y. Gladyr, A. P. H. Gelissen, O. Mergel, D. V. Pergushov, I. N. Kurochkin, F. A. Plamper, W. Richtering, *Biomacromolecules* **2014**, *15*, 3735.

[18] a) S. Wiese, A. C. Spiess, W. Richtering, *Angew. Chem. Int. Ed.* **2013**, *52*, 576; *Angew. Chem.* **2013**, *125*, 604; b) S. Wiese, Y. Tsvetkova, N. J. E. Daleiden, A. C. Spiess, W. Richtering, *Colloids Surf. A* **2016**, *495*, 193.

[19] T. Terashima, *Encyclopedia of Polymer Science and Technology* **2013**.

[20] a) N. A. Cortez-Lemus, A. Licea-Claverie, *Prog. Polym. Sci.* **2016**, *53*, 1; b) M. A. Ward, T. K. Georgiou, *Polymers* **2011**, *3*, 1215.

[21] A. J. Schmid, J. Dubbert, A. A. Rudov, J. S. Pedersen, P. Lindner, M. Karg, I. I. Potemkin, W. Richtering, *Sci. Rep.* **2016**, *6*, 22736.

[22] A. M. Rumyantsev, R. A. Gumerov, I. I. Potemkin, *Soft Matter* **2016**, *12*, 6799.

[23] R. A. Gumerov, A. M. Rumyantsev, A. A. Rudov, A. Pich, W. Richtering, M. Moller, I. I. Potemkin, *ACS Macro Lett.* **2016**, *5*, 612.

[24] H. Jia, D. Schmitz, A. Ott, A. Pich, Y. Lu, *J. Mater. Chem. A* **2015**, *3*, 6187.

[25] I. P. Beletskaya, A. R. Khokhlov, E. A. Tarasenko, V. S. Tyurin, *J. Organomet. Chem.* **2007**, *692*, 4402.

[26] a) I. M. Okhapkin, E. E. Makhaeva, A. R. Khokhlov, *Russ. Chem. Bull.* **2006**, *55*, 2190; b) I. M. Okhapkin, L. M. Bronstein, E. E. Makhaeva, V. G. Matveeva, E. M. Sulman, M. G. Sulman, A. R. Khokhlov, *Macromolecules* **2004**, *37*, 7879; c) R. Borrmann, V. Palchyk, A. Pich, M. Rueping, *ACS Catal.* **2018**, *8*, 7991.

[27] G. C. Mills, *J. Biol. Chem.* **1957**, *229*, 189.

[28] T. C. Stadtman, *Annu. Rev. Biochem* **1990**, *59*, 111.

[29] F. Ursini, M. Maiorino, R. Brigelius-Flohe, K. D. Aumann, A. Roveri, D. Schomburg, L. Flohe, *Methods Enzymol.* **1995**, *252*, 38.

[30] J. T. Rotruck, A. L. Pope, H. E. Ganther, A. B. Swanson, D. G. Hafeman, W. G. Hoekstra, *Science* **1973**, *179*, 588.

[31] G. Mugesh, W. W. du Mont, *Chem. Eur. J.* **2001**, *7*, 1365.

[32] X. Huang, Z. Y. Dong, J. Q. Liu, S. Z. Mao, J. Y. Xu, G. M. Luo, J. C. Shen, *Langmuir* **2007**, *23*, 1518.

[33] X. Zhang, H. P. Xu, Z. Y. Dong, Y. P. Wang, J. Q. Liu, J. C. Shen, *J. Am. Chem. Soc.* **2004**, *126*, 10556.

[34] Y. Fu, J. Y. Chen, H. P. Xu, C. Van Oosterwijck, X. Zhang, W. Dehaen, M. Smet, *Macromol. Rapid Commun.* **2012**, *33*, 798.

[35] a) C. T. Li, W. Huang, L. Z. Zhou, P. Huang, Y. Pang, X. Y. Zhu, D. Y. Yan, *Polym. Chem.* **2015**, *6*, 6498; b) X. F. Cheng, Y. Jin, R. Qi, W. H. Fan, H. P. Li, X. P. Sun, S. Q. Lai, *Polymer* **2016**, *101*, 370.

[36] V. I. Lozinsky, I. A. Simenel, E. A. Kurskaya, V. K. Kulakova, I. Y. Galaev, B. Mattiasson, V. Y. Grinberg, N. V. Grinberg, A. R. Khokhlov, *Polymer* **2000**, *41*, 6507.

[37] a) F. A. L. Janssen, M. Kather, L. C. Kroger, A. Mhamdi, K. Leonhard, A. Pich, A. Mitsos, *Ind. Eng. Chem. Res.* **2017**, *56*, 14545; b) A. Imaz, J. Forcada, *J. Polym. Sci. Part A* **2008**, *46*, 2766.

[38] a) Y. Maeda, T. Nakamura, I. Ikeda, *Macromolecules* **2002**, *35*, 217; b) C. Scherzinger, Dissertation thesis, RWTH Aachen University (Aachen, germany), **2015**.

[39] Z. Pikh, V. Ivasiv, *Chem. Chem. Technol.* **2012**, *6*, 9.

[40] C. Marsden, E. Taarning, D. Hansen, L. Johansen, S. K. Klitgaard, K. Egeblad, C. H. Christensen, *Green Chem.* **2008**, *10*, 168.

[41] K. Y. Koltunov, V. I. Sobolev, V. M. Bondareva, *Catal. Today* **2017**, *279*, 90.

10.1002/anie.201901161

WILEY-VCH

Entry for the Table of Contents

COMMUNICATION

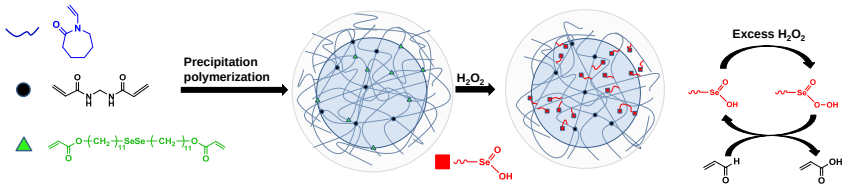

Selenium microgels: inspired by glutathione peroxidase (GPx), a mimicking of GPx approach carried out by incorporation of diselenide as crosslinks into PVCL microgels. Treatment of diselenide with hydrogen peroxide led to degradation of diselenide into seleninic acid, an oxidative functional group. The degraded microgels demonstrated high catalytic efficiency and selectivity in oxidation of acrolein at mild temperatures.

*Kok H. Tan, Wenjing Xu, Simon Stefka, Dan E. Demco, Tetiana Kharandiuk, Volodymyr Ivasiv, Roman Nebesnyi, Vladislav S. Petrovskii, Igor I. Potemkin, and Andrij Pich**

Page No. – Page No.

Selenium-Modified Microgels as Bio-Inspired Oxidation Catalysts